Virtual sound barrier for indoor transformers

Jiancheng TAO[1]; Shuping WANG[2]; Xiaojun QIU[3]; Ning HAN[4]; Linke ZHANG[5]

[1,2,3] Key Laboratory of Modern Acoustics and Institute of Acoustics, Nanjing University, Nanjing, 210093, China

[4] School of information science and engineering, Southeast University, Nanjing, 210096, China

[5]School of Energy and Power Engineering, Wuhan University of Technology, Wuhan, 430063, China

ABSTRACT

Power transformers sometimes locate in an enclosed room with an opening surface for the ventilation purpose. Under these situations, most noise radiates out from the opening, so a virtual sound barrier can be built to suppress the sound radiation outside by employing a multiple-channel active noise control system. Based on the sound radiation model of indoor monopoles, the noise reduction performances of both centralized and decentralized control systems are investigated and compared. Considering the channel number requirement, a virtual sound barrier is built for an actual indoor transformer, where both the centralized and the decentralized strategies are investigated. Simulation results show that the fully independent virtual sound barrier is effective for the indoor transformer noise control.

Keywords: Virtual sound barrier, Transformer noise I-INCE Classification of Subjects Number(s): 38.2

1. INTRODUCTION

Transformer noise is dominated by low frequency harmonic components[1], which is harmful to people and environment and hard to be controlled with traditional passive methods. Active noise control (ANC) technologies can provide better performance with low cost and easy maintenance[2-7].

For the indoor transformer locating in a cavity with one opening, a multi-channel ANC system defined as "virtual sound barrier"[8] (VSB) can be implemented at the opening to block the sound radiation outward. Although only the sound radiation through the opening needs to be considered, huge channel number is required for a large transformer, which makes the storage and computation load of the controller become too heavy to be implemented. Taking a 110 kV transformer for example, the opening area is about 48 m^2 and at least 265 channels are required considering that the control source interval should be less than a quarter of the wavelength[9] (about 0.85 m for 200 Hz). Waveform synthesis algorithms[10-11] instead of the commonly used filtered-x LMS algorithm can be used to decrease the processing power requirement; however the cross coupling between the control source and error microphones still needs to be considered.

An alternative method is to decentralize the VSB system, that is, implement many independent ANC systems instead of the multiple-input and multiple-output system. Leboucher et al. analyzed the stability of the decentralized feedback ANC system of sinusoidal sound in free space and derived practical conditions from both the small gain theorem and the Nyquist criterion[12]. Zhang et al. investigated the performance of decentralized multi-channel feedback analog control systems and obtained a sufficient stability condition in terms of the predefined maximum noise amplification and the geometrical configuration of the independent controllers[13]. It was also demonstrated that there is an optimum leakage coefficient that results in the best

[1] jctao@nju.edu.cn
[2] wangsp822105@126.com
[3] xjqiu@nju.edu.cn
[4] hanning@seu.edu.cn
[5] zhanglk1999@gmail.com

noise reduction performance and the performance decreases with the further increase of the leakage coefficient for a decentralized ANC system in the transformer noise control[14].

Besides，the feasibility of applying ANC technology on a staggered double glazing window was investigated and the measured extra noise reduction in the room is about 10 dB[15]. Sixteen independent ANC systems were installed at a 1 m^2 open window to protect the building interior from the external noise. The noise reduction of more than 10 dB was achieved for the frequency range of 200~700 Hz at the error sensors while the extra noise reduction is only 2~3 dB in the room interior[16].

Despite all the research mentioned in the preceding text, no research is found on the VSB, especially the decentralized VSB, on the opening of a cavity for interior source. This will be investigated in this paper. A theoretical model for predicting the sound radiation through the opening from the source in the cavity will be established first; then this model will be used to calculate the transfer functions employed for VSB performance evaluation. Finally the noise reduction of both decentralized and decentralized VSBs will be investigated and compared based on the numerical simulations.

2. THEORETICAL MODEL

2.1 Sound radiation from the sources in the enclosure with an opening

Figure 1 shows one primary source representing the transformer locates in an enclosure with an opening at the surface z= L_z. The enclosure dimension is $L_x \times L_y \times L_z$, and the monopole location is $\mathbf{r}_s$ (x_s, y_s, z_s) with a strength of q_0. The virtual barrier is composed by a control source array at the plane $z=L_c$ and an error microphone array at the enclosure opening. Assume that the opening is embedded in an infinite baffle and both the primary source and the control sources can be considered as monopoles, the sound pressure from one monopole source in the enclosure can be presented as

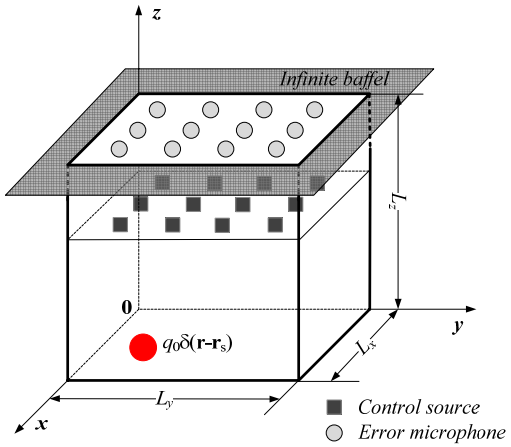

Figure 1 – Indoor monopole with a baffled opening

$$p_{\text{in}} = \sum_n \left(P_n^{\text{i}} e^{-jk_{nz}z} + P_n^{\text{r}} e^{jk_{nz}z}\right)\phi_n(x,y) + \rho_0 \omega q_0 \sum_n \frac{\phi_n(x,y)\phi_n(x_s,y_s)}{2S\Lambda_n k_{nz}} \exp\left(-jk_{nz}|z-z_s|\right) \tag{1}$$

$$p_{\text{out}} = \frac{1}{2\pi}\iint_{S_0}\sum_n \left[-\text{j}k_{nz}\left(-P_n^{\text{i}} e^{-\text{j}k_{nz}l_z} + P_n^{\text{r}} e^{\text{j}k_{nz}l_z}\right)\phi_n(x_0,y_0) - \text{j}\rho_0\omega q_0 \frac{\phi_n(x_0,y_0)\phi_n(x_s,y_s)}{2S\Lambda_n} e^{-\text{j}k_{nz}(l_z-z_s)}\right]\frac{\exp(-\text{j}kr)}{r} dS_0 \tag{2}$$

where p_{in} and p_{out} stand for the sound pressure inside and outside the cavity, P_n^{i} and P_n^{r} are the mode coefficients of the nth mode, $\phi_n(x,y)$ is the mode shape $\cos(n_x\pi/l_x)\cos(n_y\pi/l_y)$, k_{nz} is the wave number in the z direction and equals $\sqrt{k^2-(n_x\pi/l_x)^2-(n_y\pi/l_y)^2}$, k is the wave number, ω is the angular frequency, S is the opening area, ρ_0 is the air density, Λ_n is a constant depending on n_x and n_y (n_x= n_y= 0, Λ_n=1; n_x= 0 or n_y= 0, Λ_n=0.5; $n_x \neq 0$ and $n_y \neq 0$, Λ_n=0.25), r is the distance from the field point to the integration point (x_0, y_0, l_z) on the opening area S_0.

2.2 Virtual sound barrier based on active noise control

For the virtual barrier based on the ANC system, the error signals can be expressed as

$$\mathbf{e} = \mathbf{p} + \mathbf{Z}\mathbf{Q}_\mathrm{c} \tag{3}$$

where $\mathbf{p}$ is the sound pressure from the primary source, $\mathbf{Z}$ is the matrix composed by the actual transfer functions from the control sources to the error microphones and $\mathbf{Q}_\mathrm{c}$ is the strength vector of the control sources. $\mathbf{Q}_\mathrm{c}$ is normally obtained by minimizing the cost function

$$J = \mathbf{e}^\mathrm{H}\mathbf{e} + \beta\mathbf{Q}_\mathrm{c}^\mathrm{H}\mathbf{Q}_\mathrm{c} \tag{4}$$

where β is the leakage coefficient and the superscript $^\mathrm{H}$ denotes matrix transpose.

Normally, a modeling process is performed first to acquire the transfer functions of secondary paths and these transfer functions are used to calculate the error gradient in the control process. The matrix of the transfer functions of secondary paths, $\mathbf{Z}_\mathrm{e}$ is equal to the actual transfer function matrix $\mathbf{Z}$ for the fully coupled ANC system with ideal modeling condition. For the decentralized system, the values of the transfer function between the control sources and the error microphones from other independent systems are zero. If the VSB is composed by fully independent ANC systems with the same cost function and leakage coefficient as Eq. (4), $\mathbf{Z}_\mathrm{e}$ is the diagonal matrix of transfer function matrix $\mathbf{Z}$ and the off-diagonal elements are zero. Eq. (1) can thus be rewritten as

$$\mathbf{e} = \mathbf{p} + \mathbf{Z}_\mathrm{e}\mathbf{Q}_\mathrm{c} \tag{5}$$

The gradient of the const function therefore can be written as

$$\nabla J = \frac{\partial J}{\partial q_\mathrm{c}^\mathrm{R}} + \frac{\partial J}{\partial q_\mathrm{c}^\mathrm{I}} = 2\mathbf{Z}_\mathrm{e}^\mathrm{H}\mathbf{e} + 2\beta\mathbf{Q}_\mathrm{c} \tag{6}$$

where q_c^R and q_c^I are the real and image part of the control source strength. Consider the algorithm $\mathbf{Q}_\mathrm{c}(k+1) = \mathbf{Q}_\mathrm{c}(k) - \mu\nabla J$ (k is the iteration number and μ is the step size) and the system convergence condition $\mathbf{Q}_\mathrm{c}(\kappa+1) = \mathbf{Q}_\mathrm{c}(\kappa)\big|_{\kappa\to\infty}$, the control source strength can be obtained as[13]

$$\mathbf{Q}_\mathrm{c}(\infty) = -\left[\mathbf{Z}_\mathrm{e}^\mathrm{H}\mathbf{Z} + \beta\mathbf{I}\right]^{-1}\mathbf{Z}_\mathrm{e}^\mathrm{H}\mathbf{p} \tag{7}$$

It is clear that when the leakage coefficient β equals zero, the source strength can be expressed as $\mathbf{Q}_\mathrm{c}(\infty) = -\mathbf{Z}^{-1}\mathbf{p}$ and is independent on the implementation matrix $\mathbf{Z}_\mathrm{e}$. Substituting Eq. (7) into Eq. (3), the sound pressure when ANC is applied can be obtained and then the noise reduction by the virtual barrier can be evaluated by using the formulation

$$\Delta W = -10\log_{10}\left[\sum_{m=1}^{N_\mathrm{e}} e_m^2(\infty) \Big/ \sum_{m=1}^{N_\mathrm{e}} (p_m)^2\right] \tag{8}$$

where N_e is the number of evaluation points.

3. SIMULATIONS

3.1 Transfer function calculation

The proposed analytical formulation in section 2.1 has been implemented in a Matlab code. The values of L_x, L_y and L_z are 0.432 m, 0.670 m and 0.598 m. The primary source is placed at (0.12, 0.12, 0.16) m to excite the cavity modes as much as possible and the strength is 1×10^{-4} m^3/s. Besides, a boundary element model is also built in LMS Vitual Lab, and the predicted results at two random chosen field points (inside and outside the cavity) are compared with those obtained employing Eqs. (1) and (2) as shown in Figure 2.

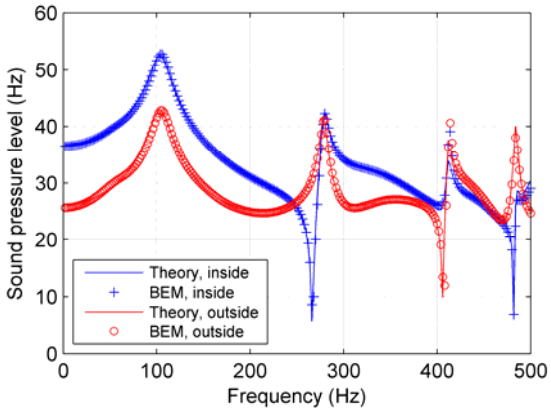

Figure 2 – Predicted sound pressure level by both analytical and boundary element methods

It is obvious from Figure 2 that the predicted sound pressure level employing the proposed analytical model agrees well with those calculated by BEM and therefore the accuracy of the proposed analytical model is validated. The value difference above 400 Hz is due to the truncation of the mode order, where only 10 modes are considered in the analytical model simulations. Another possible reason is that the element number in BEM is not sufficient at high frequencies. The transfer functions from the strength of both the primary source and the control sources to the sound pressure of field points including the error microphones are calculated based on Eqs. (1) and (2) in the following calculations.

3.2 Effect of ANC system type

As shown in Figure 1, it is assumed that 6 control sources are adopted in a horizontal plane, which is 10 cm below the enclosure opening. The nearest one to the z axis locates at (0.108, 0.1117, 0.598) m and the intervals in x and y axis are 0.216 m and 0.223 m. The error microphones are usually paired with the control sources, and they are placed at the enclosure opening and 10 cm above the control sources accordingly. 380 intersections of evenly distributed longitude and latitude lines on a semi-sphere surface are chosen for noise reduction performance evaluation. The semi sphere centers at the opening center and the radius is 10 m. It is known that the noise reduction decreases with the increase of the leakage coefficient β in general. The reason is that the control source strengths drift away from the optimum value which can be obtained when the leakage coefficient increases.

The VSB can be implemented with two different control strategies, fully coupled (6 channel centralized), and fully independent, where β is set as 0 or a randomly chosen value 1×10^7. For the fully independent VSB, each control source and the error microphone above it constitute one independent ANC system. The performance with different type VSBs is presented in Figure 3.

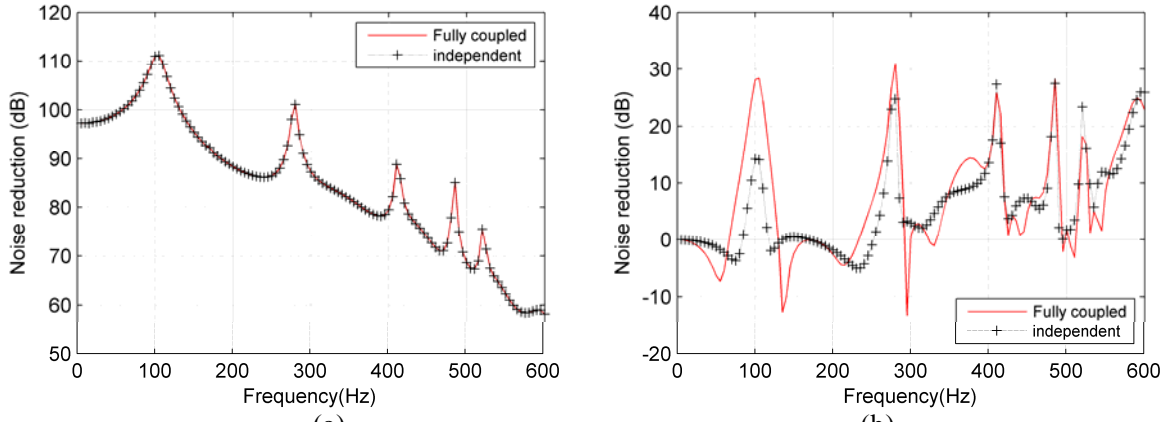

Figure 3 – Noise reduction performance of different type VSBs (a) β is zero (b) β is 1e7

It is clear from Figure 3(a) that when the leakage coefficient equals zero, the noise reduction performance is the same for both fully coupled and independent VSBs. The reason is that the control

source strength in Eq. (5) can be expressed as $\mathbf{Q}_c(\infty) = -\mathbf{Z}^{-1}\mathbf{p}$, which has no relationship with the implementation transfer function matrix $\mathbf{Z}_e$. It is also presented that the noise reduction decreases with the frequency in general while the noise reduction peaks occurs at the frequencies of the radiated sound power, such as 104 Hz, 280 Hz, 415 Hz and so on. When the leakage coefficient equals 1×10^7, the noise reduction is depressed and mainly appears at the peak frequencies of the sound power. The noise reduction performance of the fully coupled VSB is better than that of the independent VSB, while the noise amplification of coupled VSB is also larger at the frequencies around 135 Hz, 295 Hz, 425 Hz and so on, which are little higher than the peak frequencies of the sound power.

In practical applications, the noise spectrum after broadband control is almost flat and the maximum noise reduction at the original noise peaks is usually below 30 dB when the ANC system is turned on due to the background noise and the sound radiation characteristic of normal sources. Therefore it is assumed that the noise spectrum when the fully coupled VSB is implemented remains a constant value over the frequency band. This assumption is realized by optimizing the leakage coefficient for each frequency. The constant noise level is set as 32.2 dB, which is the minimum sound power above 70 Hz and the reduction at the noise peaks is about 20 dB in the simulation. The VSB is turned off and the control source strength is set to be zero when the frequency is below 70 Hz. The sound noise reduction of the independent VSB with the optimized leakage coefficient is plotted in Figure 4.

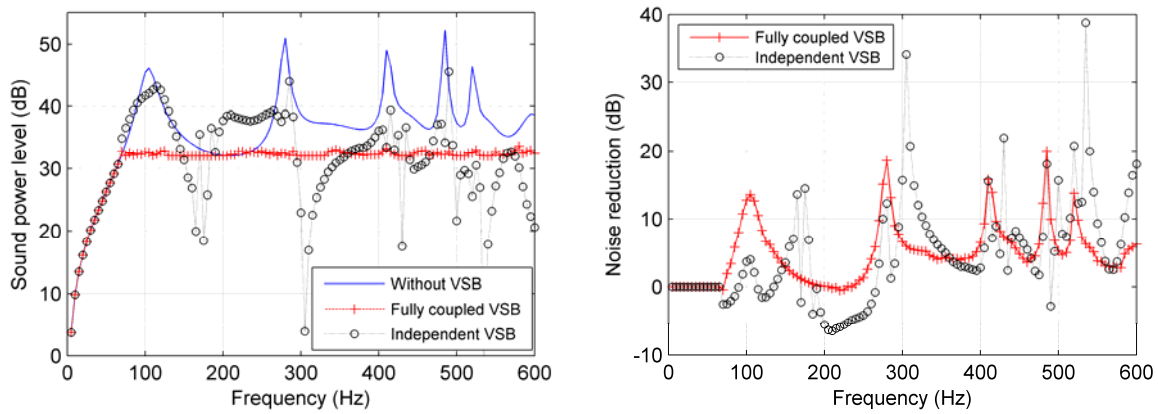

Figure 4 – Noise reduction performance of different type VSBs with optimized β

It is clear from Figure 4 that the when the noise reduction of the independent VSB is poorer than that of the fully coupled VSB in general. It can also be found that the independent VSB induces the noise amplification in the frequency band between 200 Hz and 260 Hz. The sound pressure level at six error microphones at 250 Hz is presented in Figure 5, where it is obvious that the sound pressure at all the error microphones is enhanced when the independent VSB is applied while the sound pressure reduction at error microphones is difficult to distinguish. This means that the reason for the noise amplification of independent VSB is the noise reduction criterion for leakage coefficient determination based on coupled VSB is too low at the frequencies from 200 Hz to 260 Hz.

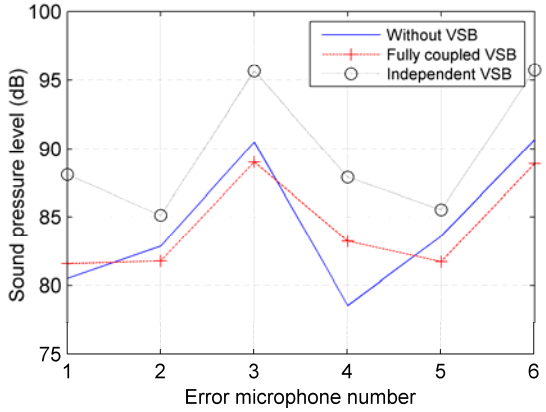

Figure 5 – Sound pressure level at the error microphones when the peak noise reduction is 20 dB

When the noise reduction criterion is enhanced to 30 dB for noise peaks, the sound noise reduction of the independent VSB with the optimized leakage coefficient is plotted in Figure 6. It is clear that the noise can be depressed at frequencies from 200 Hz to 260 Hz. Consider the results in Figure 4, it can be concluded that when the radiated noise level is high enough (30 dB above the background noise level), the independent VSB can effectively reduce the sound radiation from the indoor sound source at most frequency; when the noise level is low, the independent VSB may amplify the noise at the frequencies where the valley of the radiated sound power occurs. It may also be noted that there still exists some noise amplification in the frequency range 35 Hz to 80 Hz for the independent VSB and the reason needs to be investigated further.

It is also found that in both Figures 4 and 5 that the performance of the fully coupled VSB is better at the frequencies where the peaks of the radiation power appear. When the 20 dB criterion is adopted, the noise reduction is 9.5 dB, 5.4 dB higher compared to the independent VSB at 105 Hz and 280 Hz. When the 30 dB criterion is adopted, the noise reduction is 10.4 dB and 15.1 dB higher accordingly.

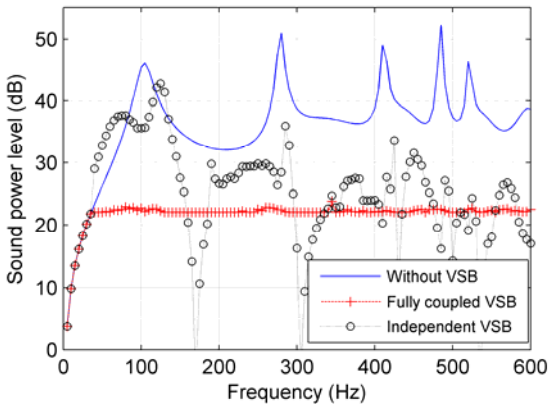

Figure 6 – Sound pressure level at the error microphones when the peak noise reduction is 30 dB

4. CONCLUSIONS

A theoretical mode for predicting the sound radiation through the opening from a monopole source in an enclosure is established and the performance of both centralized and decentralized virtual sound barrier at the opening surface is investigated. It is shown that the independent virtual sound barrier is effective at most frequencies although the noise reduction is at least 5.4 dB lower than that of the fully coupled one at the frequencies where the sound power peaks appear. Besides, there exists a noise amplification risk at the frequencies where the radiated sound power is not high enough. The feasibility of applying the decentralized virtual sound barrier for indoor transformer is validated and experimental validations needs to be further investigated.

ACKNOWLEDGEMENTS

The work is supported by the National Natural Science Foundation of China (11104141).

REFERENCES

1. Ming RS, Pan J, Norton MP, Wende S, Huang H. The sound field characterisation of a power transformer. Appl Acoust. 1999;56(4):257-272.
2. Conover WB. Fighting noise with noise. Noise Control. 1956;2:78-82.
3. Ross CF. Experiments on the active control of transformer noise. J Sound Vib. 1978;61:473-480.
4. Hesselmann N. Investigation of noise reduction on a 100 kVA transformer tank by means of active methods. Appl Acoust. 1978;11:27-34.
5. Angevine OL. Active cancellation of the hum of large electric transformers. Proc INTER-NOISE 92; 1992; Toronto, Canada 1992. p. 313-6.

6. Martin V, Roure A. Active noise control of acoustic sources using spherical harmonics expansion and a genetic algorithm simulation and experiment. J Sound Vib. 1998;212(3):511-523.
7. Qiu X., Zhang LM, Tao J. Progress in research on active control of transformer noise. Proc INTER-NOISE 2012; 19-22 August 2012; New York, USA 2012.
8. Zou H, Qiu X, Lu J, Niu F. A preliminary experimental study on virtual sound barrier system. J Sound Vib. 2007;307(1):379-385.
9. Nelson PA, Curtis ARD, Elliot SJ, Bullmore AJ. The minimum power output of free field point sources and the active control of sound. J Sound Vib. 1987;116(3): 397-414.
10. Qiu X, Hansen CH. An algorithm for active control of transformer noise with online cancellation path modelling based on perturbation method. J Sound Vib. 2000;240(4):647-65.
11. Qiu X, Li X, Ai YT, Hansen CH. A waveform synthesis algorithm for active control of transformer noise: implementation. Appl Acoust. 2002;63:467-479.
12. Leboucher E, Micheau P, Berry A, L'Espérance A. A stability analysis of a decentralized adaptive feedback active control system of sinusoidal sound in free space. J Acoust Soc Am. 2002;111(1):189-99.
13. Zhang L, Tao J, Qiu X. Performance analysis of decentralized multi-channel feedback systems for active noise control in free space. Appl Acoust. 2013;74:181-8.
14. Cordioli JA, Hansen CH, Li X, Qiu X. Numerical evaluation of a decentralised feedforward active control system for electrical transformer noise. International J Acoust Vib. 2002;7(2):100-4.
15. Huang H, Qiu X, Kang J. Active noise attenuation in ventilation windows. J Acoust Soc Am. 2011;130(1):176-88.
16. Ise S. The boundary surface control principle and its applications. IEICE Trans. Fundamentals E88-A. 2005;1656-64.